Julián Segura Rodríguez

Membranes with amine-free carboxylate ionic liquid additives for efficient CO_2 separation

MASTER'S DEGREE THESIS

Supervised by Dr. Alberto Puga

MASTER'S DEGREE IN NANOSCIENCE, MATERIALS AND PROCESSES

UNIVERSITAT ROVIRA i VIRGILI

TARRAGONA

2021

Membranes with amine-free carboxylate ionic liquid additives for efficient CO_2 separation

Julián Segura Rodriguez
Master Program in Nanoscience, Materials and Processes, 2020-2021

e-mail: julian.segura@estudiants.urv.cat

Supervisor: Alberto Puga.
Department of Chemical Engineering. Universitat Rovira i Virgili Campus Sescelades, c/. Marcel·lí Domingo, s/n Tarragona, 43007, Spain.

Abstract: Carbon capture and utilization is currently considered one of the most interesting strategies to reduce CO_2 as it involves its transformation into fuels and chemicals, reducing the extraction of fossil carbon, thus preserving resources. Among the technologies used to capture CO_2 in post-combustion processes, membranes stand out due to their low cost, high energy efficiency, and simplicity to adapt into different modules. Amine-based additives have been used to increase the solubility and the efficiency to separate CO_2 using the membranes. However, these kinds of additives demand high energy for the regeneration step due to their high CO_2 affinity. Ionic liquids (IL) have been listed as potential substitute additives since they have lower volatility, are non-flammable, are more thermally stable and easier to recycle preserving their efficacy in capturing selectively CO_2 and can be designed to require lower regeneration energy. In this work, tetrabutylphosphonium acetate hydrate ($[P_{4\,4\,4\,4}][AcO]\cdot H_2O$) is used as an ionic liquid additive to impregnate the pores of a polymeric polysulfone (PSf) membrane and increase the CO_2 solubility and selectivity. Impregnated and non-impregnated membranes are characterized by Scanning Electron Microscope (SEM) and infrared spectroscopy (FTIR). The ionic liquid was prepared by acid-base neutralization reaction and characterized by ^1H NMR. The solubility and permeability of impregnated membranes were tested from pure CO_2 gas in a steel module setup. Furthermore, performance was compared to a commercial amine-based competitor CO_2 sorbent (PEI).

Introduction

Production models have radically changed since the industrial revolution in the late eighteenth century and as a consequence, energy consumption and production have continuously increased. This change also implied an increase in the use of fossil fuels and directly related to this, an increase in greenhouse gas emissions. Among the emissions caused by human action, atmospheric CO_2 levels have dramatically risen over the last decades to the present times reaching a tipping point where it is crucial to reduce its concentration in the atmosphere, which contributes to 60% of global warming due to greenhouse effects[1–3].

Several strategies can be adopted to reduce CO_2 emissions. The most ambitious options in this context involve avoiding or minimising CO_2 emissions (using renewable electricity as major primary energy source), promoting renewable carbon (biofuels), or developing more efficient and less polluting fossil carbon technologies (combined cycle power plants, improving energy efficiency, etc.). However, decarbonisation of human activities is a challenging task and transition from the current scenario will require long implementation times, large investment efforts, and extensive research. In the meantime, fossil fuels use will continue to play a significant (yet

declining) role. Therefore, carbon capture and utilization (CCU) is the most attractive method to complement the strategies mentioned above and counterbalance CO_2 emissions during transition to a cleaner energy model.

Carbon Capture and Utilization involves the conversion of CO_2 into fuels and chemicals. It is a truly circular carbon economy strategy. Therefore, it is carbon neutral and would reduce the exploitation of fossil carbon, preserving resources and reducing at the same time CO_2 emissions[4].

Regarding CO_2 capture, a number of technologies are known, namely aqueous amine absorption, aqueous alkaline absorption, solid carbonate looping, physically adsorbent solids, or amine-impregnated sorbent solids[5,6]. These sorption-desorption methods often present some drawbacks, especially high energy consumption for regeneration and limited stability, resulting in high cost of the recovered CO_2[5–7].

Membrane-based methods are very attractive for gas separation and capture in post-combustion processes. As compared to the widely used absorption and adsorption methods, which require large industrial infrastructures and high energy costs, membrane technologies are simple to implement, scalable, compact, portable, energy-efficient, and cost-effective. In short, membranes are versatile and can be readily adapted to a large variety of modules and setups[8–10].

Previous work by our group demonstrated the efficacy of polysulfone (PSf) membranes for CO_2 capture[11]. In this study, Nogalska et al. reported the preparation of PSf membranes by casting solutions in different solvents and found that membranes obtained from 1-methyl-2-pyrrolidone (or *N*-methyl-2-pyrrolidone, NMP) solutions exhibited an appropriate morphology with large surface area due to the presence of asymmetric finger-like pores. These pores can be filled with additives to increase the solubility, permeability, and selectivity of CO_2[9,12].

Amine-based membranes are attracting significant attention due to their high affinity with CO_2, which enables a facilitated transport mechanism. This results in good carbon dioxide permeability, and high carbon dioxide/nitrogen selectivity. The current membrane technologies for CO_2 capture use additives based on different amines such as monoethanolamine (MEA), diethanolamine (DEA) or polyethylenimine (PEI). However, for CO_2 capture and utilization purposes, amine-based membranes still require a strong driving force for permeation given the high energy required for CO_2 desorption[5,7,13,14].

Recently, Ionic liquids (ILs) have been proposed as an alternative to amine-based additives because of their many advantages for the capture and subsequent desorption of CO_2 in post-combustion processes[15,16]. First, ILs can be designed for lower regeneration energy by adjusting the acid-base properties of their constituent ions[17]. Moreover, they cause minimal volatility issues due to their negligible vapor pressure. Furthermore, ILs are non-flammable and more thermally stable[5]. The result of these properties is the avoidance of contamination in the gas streams because of the absence of additive losses during the sorption and regeneration process, making regeneration a simpler process. Either increasing the temperature or decreasing the pressure, the carbon captured can be safely regenerated[16].Thus, ionic liquid-based additives are very attractive for post-combustion applications where the gas streams are usually under harsh conditions.

Cations and anions can be combined creating many different ionic liquid compounds depending on their structures. Symmetry, size, presence of functional groups, chain length or branching are some examples of structural parameters which can be modified. All of these changes can strongly affect their physical and chemical properties, and thus, their interaction with CO_2. Carbon dioxide can be absorbed physically and/or chemically[16,18–20].

Due to the strong interaction between CO_2 and amines, many authors functionalized ILs with these groups, achieving high CO_2 solubilities. However, these functionalized ionic liquids still have some of the drawbacks of aqueous amine sorbents mentioned above. These amine functionalized compounds have high enthalpies of absorption and high regeneration temperatures increasing the energy required in the regeneration step[21,22].

Remarkable solubility of CO_2 in carboxylate, chiefly acetate, ionic liquids was reported by several research groups[23–25]. Kirchner *et al.* demonstrated the strong acid-base interaction between the acetate anion and CO_2[26]. Moreover, Luebke *et al*[27] simulated the interaction between $[P_{4\,4\,4\,4}][AcO]$ and CO_2 and demonstrated the strong nonphysical interaction of the acetate anion with CO_2. Furthermore, acetate compounds may be accepted in the industry since they are environmentally friendly and affordable [2].

The cation of the IL has also a key role in the CO_2 capture since increasing the cation alkyl side chain length increases CO_2 solubility. However, if the alkyl chain is too large, the molar equivalence between the IL and CO_2 decrease, and thus, solubility also decreases[5].

Phosphonium-based ILs are generally more thermally stable than ammonium counterparts. Pena et al. studied the thermostability of tetrabutylphosphonium acetate ($[P_{4444}][AcO]$), observing a decomposition temperature of 317ºC[1]. A similar ammonium IL (triethylbutylammonium acetate) showed an equivalent onset of thermal degradation at 171 ºC[28]. Moreover, Pena and co-workers demonstrated the chemical interaction between $[P_{4444}][AcO]$ and CO_2 and considered it as a promising solution for CO_2 capture[2]. Wang *et al* [29] simulated the CO_2/N_2 selectivity of this ionic liquid and demonstrated a high theoretical adsorption selectivity for CO_2.

It is interesting to note that chemical absorption is enhanced by the hydrated IL ($[P_{4444}][AcO]\cdot H_2O$) due to the favorable formation of bicarbonate as a product in a reversible process, resulting in a maximum theoretical capacity of 1 mol(CO_2)/mol(IL)[30] (Figure 1). In summary, $[P_{4444}][AcO]\cdot H_2O$ is selected herein as an additive for CO_2 separation membranes, since it is composed of an anion that has strong interaction with CO_2, and a cation with long enough alkyl chains for suitable CO_2 capture and preventing crystallisation, but not as long to decrease the solubility.

In this work, a porous polysulfone (PSf) membrane is developed as an appropriate support material for CO_2 capture. Furthermore, PSf membranes are impregnated with $[P_{4444}][AcO]\cdot H_2O$ to increase the CO_2 permeability and selectivity (Figure 1)[30]. The solubility, selectivity, and permeability of IL-membranes are studied and compared with the current commercial additives based on amines. It is expected to reach a similar CO_2 capture capacity but with lower energy requirement in the regeneration step since ILs have a lower enthalpy of CO_2 absorption[5,31,32].

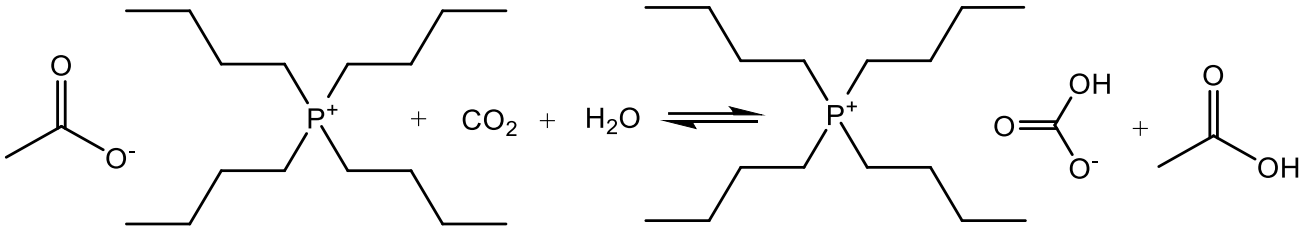

Figure 1. Reversible ionic liquid-CO_2 chemical absorption reaction involving $[P_{4444}][AcO]\cdot H_2O$ and resulting in the formation of bicarbonate as the captured species.

Experimental section

Materials

Polysulfone (PSf, MW 35000 Da) in a transparent pellet form, tetrabutylphosphonium hydroxide solution (40% wt. in H_2O) and polyethylenimine branched (PEI) were purchased from Sigma-Aldrich. *N*-methyl-2-pyrrolidone (NMP), *N*,*N*-dimethylformamide (DMF), and acetic acid were purchased from Scharlab. Methanol (99% purity) was purchased from Merck. High-purity CO_2 (> 99.995%) was obtained from Carburos Metálicos.

Membrane preparation

Membranes were prepared in ambient conditions by phase inversion precipitation using polysulfone as polymer and either NMP or DMF as solvents. According to a previous work by our group reporting the preparation of PSf membranes having asymmetric finger-like pores, 20% PSf/NMP and 20% PSf/DMF (w/w) solution were prepared[11]. These solutions were stirred for 48 hours in ambient conditions and then sonicated for 2 hours before membrane preparation, to remove any dissolved or trapped air.

The resulting homogeneous solutions were cast over a rectangular glass with a casting knife having a 250 µm gap. After casting, and rapidly, the glass was immersed in the coagulation bath (deionised water), which dissolves the organic solvent and causes the formation of a flat sheet of polysulfone membrane on the glass. Polysulfone membrane is left for 15 minutes in the coagulation bath and then rinsed with water to remove the excess solvent. Membranes were left overnight in air to dry. The morphology of the membranes depends mainly on the speed of precipitation and on the organic solvents, among other precipitation conditions.

Synthesis of Ionic Liquid

Tetrabutylphosphonium acetate ($[P_{4444}][AcO]$) preparation was based on an acid-base neutralization method. Acetic acid was weighted and dissolved in deionised water (≈3.5 g, ≈58 mmol). Then, an equimolar amount of tetrabutylphosphonium hydroxide, as previously calculated, (≈ 40 mL, 40% w/w, ≈58 mmol) was added until the final molar equivalence point (pH = 8.99). The pH was measured in real time using a Metrohm pH meter. The total final volume of the solution was 200 mL. The solution was stirred for 24 hours under ambient conditions.

Water was evaporated until a molar ratio of 1:1 (H_2O/IL) in order to increase the CO_2 sorption capacity and maintain a reasonable viscosity of the sorbent. The removal of water was performed using a rotatory evaporator at 60ºC (bath temperature) and under low pressure around 20 mbar.

The final water content was measured by Karl-Fischer analysis and was adjusted to ≈ 1 mol(H_2O)/1 mol(IL).

The colourless viscous IL hydrate was stored under N_2 atmosphere and moisture to avoid the absorption of CO_2 from air.

Membrane impregnation

$[P_{4444}][AcO]\cdot H_2O$ and its commercial amine-based competitor (PEI) were diluted in methanol to reduce their viscosity and facilitate their impregnation. 20 mL of each solution were prepared, in the case of IL was 33,3% concentrated and for PEI it was only 3,6%). The PEI solution was diluted in order to have only 20% of content of PEI respect the IL, which was 100%, and hence, have two comparable impregnated membranes with a similar theoretical sorption capacity (≈1.5 mmol(CO_2)/g(liquid sorbent)[33].

Polysulfone membranes prepared from NMP solutions were cut with a circular shape of 16 cm^2 of area and were impregnated with $[P_{4444}][AcO]\cdot H_2O$ or PEI under vacuum conditions to help the liquid fill the pores of the membrane. Membranes were immersed in the methanolic solutions (containing either ionic liquid or amine sorbent) and under vacuum conditions at room temperature. The vacuum was left until the membrane stopped bubbling (approx. 1 minute) and then was left under N_2 atmosphere for 30 min to avoid the absorption of CO_2 from air.

After this time, membranes were removed from the solution and dried at 60ºC on Petri dishes inside an oven until a constant weight. The amount of additive impregnated in the membrane was determined gravimetrically by weighting the membranes before and after impregnations. Table 1 shows the average values of the impregnation weights.

Table 1. Additive weights of impregnated membranes.

Additive	Initial weight (g)	Final weight (g)	Impregnated additive (g)	Impregnated additive (%)
IL	0,145	0,2209	0,0759 ± 0,006	52,3 %
PEI	0,229	0,244	0,0117 ± 0,003	5,1 %

Then, the resulting PSF-IL and PSF-PEI membranes were stored in a desiccator under anhydrous conditions until further use.

Characterization methods

Environmental Scanning Electron Microscope (ESEM) was used to study the morphology, thickness, and porosity of polysulfone membranes. A sample of the membrane was cut and immersed into liquid nitrogen and fractured. Cross-section micrographs were taken and were analysed by ImageJ software. Impregnated membranes were analysed by Field Emission Scanning Electron Microscope (FESEM). Furthermore, impregnated membranes were examined by Energy-Dispersive X-ray spectroscopy (EDX) to study the composition and distribution of the additives.

The porosity of membranes was calculated using the following equation:

$$\varepsilon = \left(1 - \frac{P_m}{P_{PSf}}\right) \quad (1)$$

where ε is the porosity coefficient and was expressed in percentage, P_m is the overall density of the membrane (also considering the pore volume), determined by cutting a piece of membrane (1 cm^2) and dividing its weight by its volume, as calculated by considering uniform thickness (determined by ESEM) and P_{PSf} is the density of bulk polysulfone [g/cm^3].

Attenuated Total Reflectance Fourier-Transform Infrared (ATR-FTIR) spectra were recorded on a Jasco FT/IR instrument and processed using the Spectra Manager™ Suite Spectroscopy Software by Jasco Corporation. This was done to confirm the chemical composition of the membranes. The spectra were collected in the wavelength range of 400-4000 cm^{-1} in the absorbance mode.

The structure of the ionic liquid was confirmed after synthesis by ^1H NMR spectroscopy on a Varian Gemini 400 spectrometer (400 MHz) using dimethyl sulfoxide-d_6 (dmso-d_6) in a sealed capillary tube as an external standard.

Solubility and permeability tests

Solubility tests were performed using a stainless-steel module which contains 0.150 g of material (PSf, PSf-IL, or PSf-PEI membranes). Fig. 2 shows a schematic representation of the set-up used for solubility tests. Before experiments, the internal air from module and channels was removed by applying vacuum. Then, when the pressure was near zero around (0,3 bar) , the three-way valve (3) was turned over and pure CO_2 was introduced into the system. When the pressure reached 2 bar (equal to the CO_2 line, as adjusted by a pressure regulator), the valve was closed. The solubility was studied by measurements of pressure decay by using a digital UPS-HSR USB Pressure Sensor (Stork Solutions).

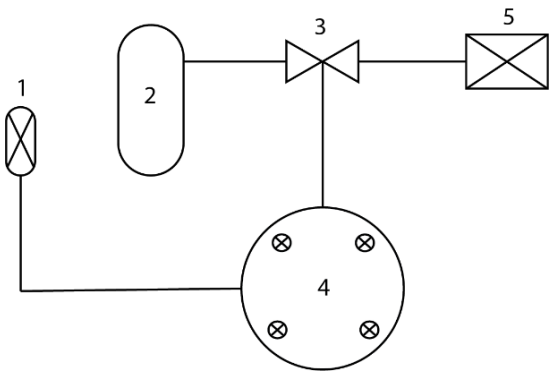

Figure 2. Experimental CO_2 solubility set-up. 1) Pressure sensor 2) CO_2 gas bottle 3) Valve 4) Steel module containing membrane 5) Vacuum system.

The solubility was calculated following the same procedure as a described in a previous study by our group[11] according to the following equation:

$$n = \frac{(p_i - p_f)\cdot V}{R\cdot T} \quad (2)$$

Where n is the adsorbed moles of CO_2, p_i is the maximum pressure value before decaying and p_f is the final pressure where it was stabilized [Pa], V is the total volume of the system [m^3], R is the gas constant (8,314 [J/K/mol]) and T is temperature [K]. Total volume was estimated introducing a known quantity of gas into the module at a defined pressure (> 1 bar), closing the valve, and opening another valve that connects to a volumetric syringe that was filled with the internal gas until pressure equilibration and reading the filled volume on the syringe.

The solubility coefficient (S_{CO2}) was expressed according to the following equation (3).

$$S_{CO2} = \frac{V_{CO2m(STP)}}{V_m \cdot P_{established}} \quad (3)$$

where V_{CO2m} *(STP)* is the volume of CO_2 corresponding to n_{CO2} at standard conditions [m^3], V_m is the material total volume [m^3], also considering the free space from the pores, and $P_{established}$ is the pressure at equilibrium conditions [atm].

The solubility coefficient was expressed in [m^3(STP)/m^3 PSf atm] units.

Gas permeation tests were measured using the same stainless-steel module but with different set-up. For these experiments, instead of using cropped material, circular membranes with a diameter around 4,6 cm were used. Fig. 3 shows a schematic representation of the set-up. Now, the membranes under study were placed at the centre of the module between the feed and permeate compartments, leaning on a circular pierced steel support to avoid damage to the membrane due to pressure gradient. Sealing was ensured using an appropriate rubber O-ring. Pure CO_2 was introduced continuously in the system. The increase of pressure in the permeate side of the module was measured using the pressure sensor (5).

The experiments were performed for 2 hours while keeping the pressure of CO_2 in the feed at 2 bars. Pressure was recorded versus time. The slope of the curve will define the permeability of the materials. Permeability coefficients were calculated from the slopes of the curves of the increase of pressure in the permeability tests described above. Coefficients were expressed in *mol/(cm^2·kPa·s)* where *mol* are CO_2 mols calculated from the difference of pressure between minutes 5 and 25, *cm^2* is the area of the membrane, *kPa* is the pressure in minute 5 and *s* is the time between these two points.

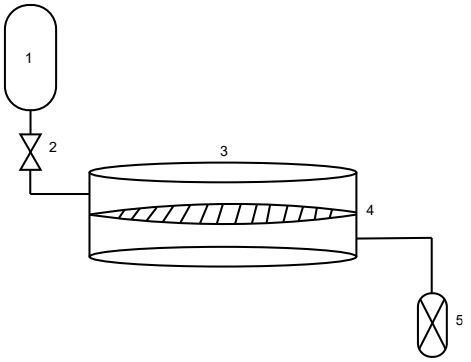

Figure 3. Experimental CO2 permeability set-up. 1) CO_2 gas bottle 2) Valve 3) Steel module containing membrane 4) Membrane 5) Pressure sensor.

Results and discussion

Membrane preparation

The relationship between the membrane material and the composition of the coagulation bath determines the velocity of membrane formation, and hence, morphology. The aim is to get asymmetric finger-like pores in PSf membranes and then fill the pores with the additive and increase their sorption capacity. The thickness has also a key role in this study since the permeability will depend on the ease of gas going through the membrane. Figure 4 shows a cross-section image taken by ESEM from the polysulfone membranes made with NMP and DMF.

In Figure 4a, asymmetric voids can be observed through the membrane prepared from an NMP solution. Furthermore, on the top side of the membrane, the pores reach the surface. For the impregnation step, this characteristic of the membrane morphology is key because this side of the membrane will readily provide access for the ionic liquid (or other liquid sorbent) to go inside the pores. Figure 4b shows the cross-section image

from the membrane made with polymer dissolved in DMF. In this case, symmetric sponge-like pores can be observed.

Even though having similar porosity (Table 2), membranes made with DMF seem less attractive because these types of pores make the membrane less accessible for the viscous ionic liquid since the size average of the diameter of porous is around 1 µm while the channels of the finger-like membrane are around 10 µm. Regarding the thickness, membranes made with NMP are slightly thicker than membranes made with DMF (Table 2). Moreover, the finger-like morphology of the channels in the membrane prepared from NMP is expected to enable a more facile diffusion of gas across the membranes. Filling these finger-like pores with a sorbent liquid selective to CO_2 should facilitate its transport. For these reasons, membranes for impregnation and further studies were prepared from solutions in NMP.

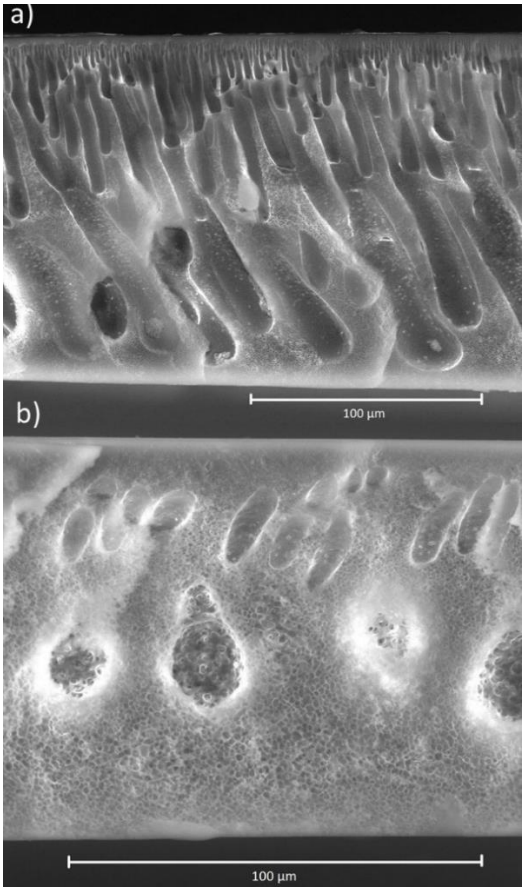

Figure 4. ESEM micrographs of the cross-sections of , a) PSf membrane from 20% solution in NMP, b) PSf membrane from 20% solution in DMF.

Synthesis of Ionic Liquid

After the synthesis of tetrabutylphosphonium acetate, its structure was confirmed by ^{1}H NMR spectroscopy. The spectrum in Figure 6 shows the value of the integration of each peak. Also, it helped to determine the molar ratio of water in the as-prepared IL, which was adjusted later to 1 equivalent of water, and checked by Karl-Fischer titration.

Table 2. Porosity and thickness of resulting PSf membranes.

Membrane solvent	**Porosity, ε**	**Thickness**
NMP	75,3 %	192,5 µm
DMF	78,8 %	165 µm

Membrane impregnation

Figure 5 shows a FESEM micrograph of IL-impregnated polysulfone (PSf-IL) made from NMP solution. The conductive character of the ionic liquid made possible the use of FESEM and reach this magnitude of resolution. In this micrograph, symmetric sponge-like micropores (≈ 1 µm) can be observed in addition to the larger finger-like channels (up to 20 µm wide) of the membrane. After the impregnation with ionic liquid the morphology of the membrane does not change.

Table 3. Loading of IL or PEI in the impregnated membranes.

Membrane	**Loading (wt% as IL or PEI vs. PSf) by gravimetry**	**Atomic ratio (P/S or N/S) by FESEM-EDX**	**Loading (wt% as IL or PEI vs. PSf) by FESEM-EDX**
PSf-IL	52,5	0,39 ± 0,04	30 ± 3
PSf-PEI	5,1	1,7 ± 0,2	16 ± 2

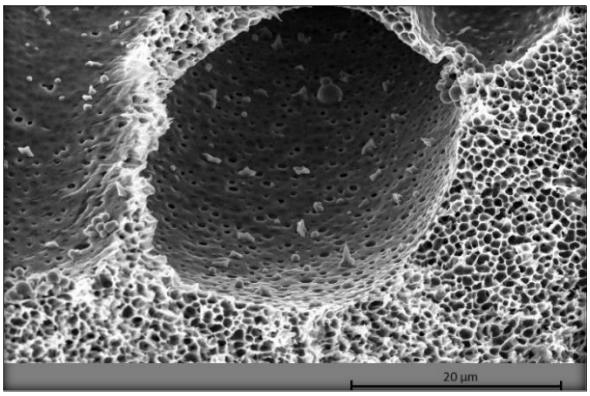

Figure 5. FESEM micrograph of polysulfone membrane made from NMP solution and then impregnated with tetrabutylphosphonium acetate (PEI-IL).

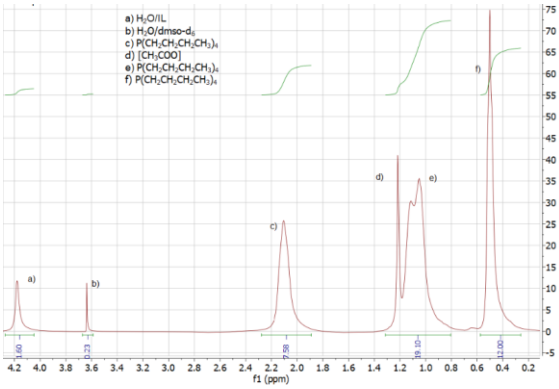

Figure 6. ^1H NMR spectrum of $[P_{4\,4\,4\,4}][AcO]{\cdot}H_2O$ (dmso-d6 external standard, 400 MHz, 25 °C).

Elemental analysis by EDX spectroscopy integrated in the FESEM indicates the presence of the additives in the membranes. Figure 7 shows the EDX spectra for the three studied membranes. The first spectrum (a) is from polysulfone without additives where it can be observed two predominant peaks due to carbon and oxygen and a smaller one due to sulphur. The second spectrum corresponds to polysulfone membrane impregnated with $[P_{4\,4\,4\,4}][AcO]{\cdot}H_2O$ (PSf-IL). A new peak due to phosphorus is clearly observed, indicating the presence of the ionic liquid in the membrane. The last spectrum corresponds to polysulfone membrane impregnated with polyethylenimine (PSf-PEI). The nitrogen peak should be observed, but the amine loading is lower (Table 3) the impregnation step in order to have similar CO_2 solubility results than for ionic liquid membranes. The higher PEI loading value in FESEM-EDX could be due to an error because of the weakness of the signal of N, this value could be overestimated.

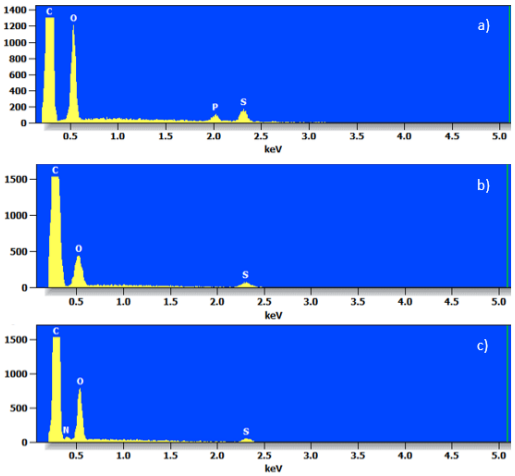

Figure 7. FESEM-EDX spectra from: a) Polysulfone (PSf) membrane, b) Polysulfone membrane impregnated with IL (PSf-IL), c) Polysulfone membrane impregnated with PEI (PSf-PEI).

Infrared spectra also confirm the impregnation of IL in the membrane comparing the spectrum from impregnated polysulfone membrane with the spectrum from IL (supplementary data S1). The clearest peak that confirms the presence of IL in the polysulfone is at 1384 cm^{-1} (carboxylate symmetric stretching) and the peak observed at 908 cm^{-1} that can be from P-C stretching. The peak around 2900 cm^{-1} also corresponds to ionic liquid.

Solubility and permeability tests

Figure 8 shows the decrease of pressure in the different membranes. To be easily compared, the initial pressure from all measurements is adjusted to 1 barg, and the rest of values are relative to this adjustment. As it can be seen in the graph, the solubility of impregnated membranes is higher than membranes without additive since the decrease of pressure is more notable. It should be noted that a higher quantity of ionic liquid than its commercial amine-based competitor was loaded on the membrane to equalise the theoretical CO_2 capacity of both sorbents (≈1.5 mmol(CO_2)/g(liquid sorbent)).

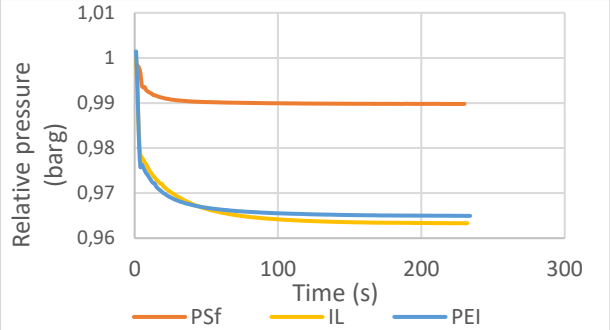

Figure 8. Decrease of pressure of membranes listed in solubility tests.

Solubility from polysulfone and impregnated membranes is expressed in Table 4. IL-impregnated membranes show almost five times more solubility capacity than polysulfone membranes.

Table 4. Solubility of resulting membranes.

Material	n_{CO2} **[mmol]**	S **[m³ STP/m³ atm]**
Polysulfone	0,06 ± 0,02	1,59 ± 0,14
PSf-IL	0,21 ± 0,07	7,88 ± 0,38
PSf-PEI	0,29	7,11

Unmodified polysulfone membranes present higher CO_2 permeability than impregnated membranes as shown in Figure 9 and in Table 5. In this graph, an increase of pressure versus time can be observed, as recorded for experiment performed as detailed in Figure 3. In this way, it is more difficult for CO_2 to go through the impregnated membranes than through unmodified membranes. This is not surprising, and we hypothesize that since there is a viscous liquid covering the channels and pores, there is less space for CO_2 to diffuse.

Table 5. Permeability of resulting membranes.

Material	**Permeability (mol/(cm² kPa s)**
Polysulfone	$7{,}87 \cdot 10^{-11}$
PSf-IL	$1{,}90 \cdot 10^{-11}$
PSf-PEI	$1{,}84 \cdot 10^{-11}$

Amine-based membranes show marginally higher permeability than ionic liquid-based membranes. This could be due to the smaller amount of additive in this kind of supporting material since there is five times less additive than in the IL-based membranes and hence, there is less viscous liquid obstructing the channels. Considering this, the permeability of the ionic liquid-based membranes is remarkably similar to that of the amine counterpart.

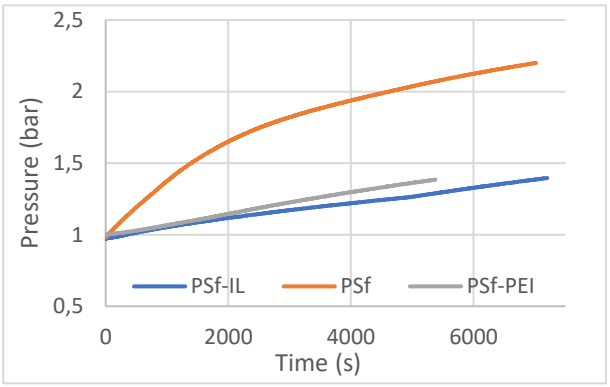

Figure 9. Increase of pressure of membranes listed in permeability tests.

Conclusions

An amine-free and a commercial amine (ionic liquid and PEI) were impregnated successfully in polysulfone membranes by simply applying vacuum and covering the membranes with the additive in less than 30 minutes. Polysulfone dissolved in NMP has been suitable for membrane preparation by coagulation in water due to the asymmetric finger-like pores observed in their cross-sections. Solubility and permeability abilities from these materials have been successfully studied with a self-made stainless-steel module. CO_2 solubility tests show that impregnated membranes have almost five times higher CO_2 adsorption abilities than unmodified polysulfone membranes. However, it has been demonstrated that the presence of these additives does not improve the permeability capacity of polysulfone. Despite the high cost of ionic liquids, it has been shown that these carboxylic based additives could be a competitor for currently used amine-based additives overcoming some drawbacks such as the poor stability and for future works it could be useful the study of the energy requirements in the regeneration step.

References

(1) Pena, C. A.; Soto, A.; King, A. W. T.; Rodríguez, H. Improved Reactivity of Cellulose via Its Crystallinity Reduction by Nondissolving Pretreatment with an Ionic Liquid. *ACS Sustain. Chem. Eng.* **2019**, *7* (10), 9164–9171. https://doi.org/10.1021/acssuschemeng.8b06357.

(2) Pena, C. A.; Soto, A.; Rodríguez, H. Tetrabutylphosphonium Acetate and Its Eutectic Mixtures with Common-Cation Halides as Solvents for Carbon Dioxide Capture. *Chem. Eng. J.* **2021**, *409* (October 2020). https://doi.org/10.1016/j.cej.2020.128191.

(3) Zare, A.; Perna, L.; Nogalska, A.; Ambrogi, V.; Cerruti, P.; Tylkowski, B.; García-Valls, R.; Giamberini, M. Polymer Blends for Improved CO2 Capture Membranes. *Polymers (Basel).* **2019**, *11* (10). https://doi.org/10.3390/polym11101662.

(4) Aresta, M.; Dibenedetto, A.; Angelini, A. Catalysis for the Valorization of Exhaust Carbon: From CO2 to Chemicals, Materials, and Fuels. Technological Use of CO2. *Chem. Rev.* **2014**, *114* (3), 1709–1742. https://doi.org/10.1021/cr4002758.

(5) Boot-Handford, M. E.; Abanades, J. C.; Anthony, E. J.; Blunt, M. J.; Brandani, S.; Mac Dowell, N.; Fernández, J. R.; Ferrari, M. C.; Gross, R.; Hallett, J. P.; Haszeldine, R. S.; Heptonstall, P.; Lyngfelt, A.; Makuch, Z.; Mangano, E.; Porter, R. T. J.; Pourkashanian, M.; Rochelle, G. T.; Shah, N.; Yao, J. G.; Fennell, P. S. Carbon Capture and Storage Update. *Energy Environ. Sci.* **2014**, *7* (1), 130–189. https://doi.org/10.1039/c3ee42350f.

(6) Leung, D. Y. C.; Caramanna, G.; Maroto-Valer, M. M. An Overview of Current Status of Carbon Dioxide Capture and Storage Technologies. *Renew. Sustain. Energy Rev.* **2014**, *39*, 426–443. https://doi.org/10.1016/j.rser.2014.07.093.

(7) Koytsoumpa, E. I.; Bergins, C.; Kakaras, E. The CO2 Economy: Review of CO2 Capture and Reuse Technologies. *J. Supercrit. Fluids* **2018**, *132* (July 2017), 3–16. https://doi.org/10.1016/j.supflu.2017.07.029.

(8) Chen, H.; Xiao, Y.; Chung, T. S. Synthesis and Characterization of Poly (Ethylene Oxide) Containing Copolyimides for Hydrogen Purification. *Polymer (Guildf).* **2010**, *51* (18), 4077–4086. https://doi.org/10.1016/j.polymer.2010.06.046.

(9) Brunetti, A.; Scura, F.; Barbieri, G.; Drioli, E. Membrane Technologies for CO2 Separation. *J. Memb. Sci.* **2010**, *359* (1–2), 115–125. https://doi.org/10.1016/j.memsci.2009.11.040.

(10) D'Alessandro, D. M.; Smit, B.; Long, J. R. Carbon Dioxide Capture: Prospects for New Materials. *Angew. Chemie - Int. Ed.* **2010**, *49* (35), 6058–6082. https://doi.org/10.1002/anie.201000431.

(11) Nogalska, A.; Ammendola, M.; Tylkowski, B.; Ambrogi, V.; Garcia-Valls, R. Ambient CO2 Adsorption via Membrane Contactors – Value of Assimilation from Air as Nature Stomata. *J. Memb. Sci.* **2018**, *546* (June 2017), 41–49. https://doi.org/10.1016/j.memsci.2017.10.007.

(12) Sun, J.; Yi, Z.; Zhao, X.; Zhou, Y.; Gao, C. CO2 Separation Membranes with High Permeability and CO2/N2 Selectivity Prepared by Electrostatic Self-Assembly of Polyethylenimine on Reverse Osmosis Membranes. *RSC Adv.* **2017**, *7* (24), 14678–14687. https://doi.org/10.1039/c7ra00094d.

(13) Tong, Z.; Ho, W. S. W. New Sterically Hindered Polyvinylamine Membranes for CO2 Separation and Capture. *J. Memb. Sci.* **2017**, *543* (June), 202–211. https://doi.org/10.1016/j.memsci.2017.08.057.

(14) Salim, W.; Han, Y.; Vakharia, V.; Wu, D.; Wheeler, D. J.; Ho, W. S. W. Scale-up of Amine-Containing Membranes for Hydrogen Purification for Fuel Cells. *J. Memb. Sci.* **2019**, *573*, 465–475. https://doi.org/10.1016/j.memsci.2018.12.022.

(15) Zeng, S.; Zhang, X.; Bai, L.; Zhang, X.; Wang, H.; Wang, J.; Bao, D.; Li, M.; Liu, X.; Zhang, S. Ionic-Liquid-Based CO2 Capture Systems: Structure, Interaction and Process. *Chem. Rev.* **2017**, *117* (14), 9625–9673. https://doi.org/10.1021/acs.chemrev.7b00072.

(16) Brennecke, J. F.; Gurkan, B. E. Ionic Liquids for CO2 Capture and Emission Reduction. *J. Phys. Chem. Lett.* **2010**, *1* (24), 3459–3464. https://doi.org/10.1021/jz1014828.

(17) Cui, G.; Wang, J.; Zhang, S. Active Chemisorption Sites in Functionalized Ionic Liquids for Carbon Capture. *Chem. Soc. Rev.* **2016**, *45* (15), 4307–4339. https://doi.org/10.1039/c5cs00462d.

(18) Ramdin, M.; De Loos, T. W.; Vlugt, T. J. H. State-of-the-Art of CO 2 Capture with Ionic Liquids. *Ind. Eng. Chem. Res.* **2012**, *51* (24), 8149–8177. https://doi.org/10.1021/ie3003705.

(19) Alkhatib, I. I. I.; Ferreira, M. L.; Alba, C. G.; Bahamon, D.; Llovell, F.; Pereiro, A. B.; Araújo, J. M. M.; Abu-Zahra, M. R. M.; Vega, L. F. Screening of Ionic Liquids and Deep Eutectic Solvents for Physical CO2Absorption by Soft-SAFT Using Key Performance Indicators. *J. Chem. Eng. Data* **2020**, *65* (12), 5844–5861. https://doi.org/10.1021/acs.jced.0c00750.

(20) Karimi, B.; Tavakolian, M.; Akbari, M.; Mansouri, F. Ionic Liquids in Asymmetric Synthesis: An Overall View from Reaction Media to Supported Ionic Liquid Catalysis. *ChemCatChem* **2018**, *10* (15), 3173–3205. https://doi.org/10.1002/cctc.201701919.

(21) Bates, E. D.; Mayton, R. D.; Ntai, I.; Davis, J. H. CO 2 Capture by a Task-Specific Ionic Liquid - JACS.Communications.01/19/2002.Pdf. **2002**, 2001–2002.

(22) Raja Shahrom, M. S.; Nordin, A. R.; Wilfred, C. D. The Improvement of Activated Carbon as CO2 Adsorbent with Supported Amine Functionalized Ionic Liquids. *J. Environ. Chem. Eng.* **2019**, *7* (5), 103319. https://doi.org/10.1016/j.jece.2019.103319.

(23) Shiflett, M. B.; Kasprzak, D. J.; Junk, C. P.; Yokozeki, A. Phase Behavior of {carbon Dioxide + [Bmim][Ac]} Mixtures. *J. Chem. Thermodyn.* **2008**, *40* (1), 25–31. https://doi.org/10.1016/j.jct.2007.06.003.

(24) Shiflett, M. B.; Drew, D. W.; Cantini, R. A.; Yokozeki, A. Carbon Dioxide Capture Using Ionic Liquid 1-Butyl-3-Methylimidazolium Acetate. *Energy and Fuels* **2010**, *24* (10), 5781–5789. https://doi.org/10.1021/ef100868a.

(25) Gurau, G.; Rodríguez, H.; Kelley, S. P.; Janiczek, P.; Kalb, R. S.; Rogers, R. D. Demonstration of Chemisorption of Carbon Dioxide in 1,3-Dialkylimidazolium Acetate Ionic Liquids. *Angew. Chemie - Int. Ed.* **2011**, *50* (50), 12024–12026. https://doi.org/10.1002/anie.201105198.

(26) Hollőczki, O.; Kelemen, Z.; Könczöl, L.; Szieberth, D.; Nyulászi, L.; Stark, A.; Kirchner, B. Significant Cation Effects

in Carbon Dioxide-Ionic Liquid Systems. *ChemPhysChem* **2013**, *14* (2), 315–320. https://doi.org/10.1002/cphc.201200970.

(27) Shi, W.; Thompson, R. L.; Albenze, E.; Steckel, J. A.; Nulwala, H. B.; Luebke, D. R. Contribution of the Acetate Anion to CO2 Solubility in Ionic Liquids: Theoretical Method Development and Experimental Study. *J. Phys. Chem. B* **2014**, *118* (26), 7383–7394. https://doi.org/10.1021/jp502425a.

(28) Wang, G.; Hou, W.; Xiao, F.; Geng, J.; Wu, Y.; Zhang, Z. Low-Viscosity Triethylbutylammonium Acetate as a Task-Specific Ionic Liquid for Reversible CO2 Absorption. *J. Chem. Eng. Data* **2011**, *56* (4), 1125–1133. https://doi.org/10.1021/je101014q.

(29) Ma, J.; Wang, Y.; Zhu, M.; Yang, X.; Wang, B. Insight into the Separation Mechanism of Acetate Anion-Based Ionic Liquids on CO2 and N2: A Multi-Scale Simulation Study. *J. Mol. Liq.* **2020**, *320*, 114408. https://doi.org/10.1016/j.molliq.2020.114408.

(30) Anderson, K.; Atkins, M. P.; Estager, J.; Kuah, Y.; Ng, S.; Oliferenko, A. A.; Plechkova, N. V.; Puga, A. V.; Seddon, K. R.; Wassell, D. F. Carbon Dioxide Uptake from Natural Gas by Binary Ionic Liquid-Water Mixtures. *Green Chem.* **2015**, *17* (8), 4340–4354. https://doi.org/10.1039/c5gc00720h.

(31) Shiflett, M. B.; Elliott, B. A.; Lustig, S. R.; Sabesan, S.; Kelkar, M. S.; Yokozeki, A. Phase Behavior of CO2 in Room-Temperature Ionic Liquid 1-Ethyl-3-Ethylimidazolium Acetate. *ChemPhysChem* **2012**, *13* (7), 1806–1817. https://doi.org/10.1002/cphc.201200023.

(32) D. Chinn, D. Q. vu, M. S. Driver, and L. C. Boudreau, "CO_2 removal from gas using ionic liquid absorbents," U.S. Patent 7527775B2

(33) Thesis, M. S. D. Mohammad Yousefe SOLID-SUPPORTED CO 2 SORBENTS BASED ON AMINE-FREE PHOSPHONIUM CARBOXYLATE IONIC LIQUIDS MASTER ' S DEGREE THESIS Supervised by Dr Alberto Puga MASTER ' S DEGREE IN NANOSCIENCE , MATERIALS AND PROCESSES : CHEMICAL TECHNOLOGY AT THE FRONTIER Tarragona. **2020**.

Supplementary data

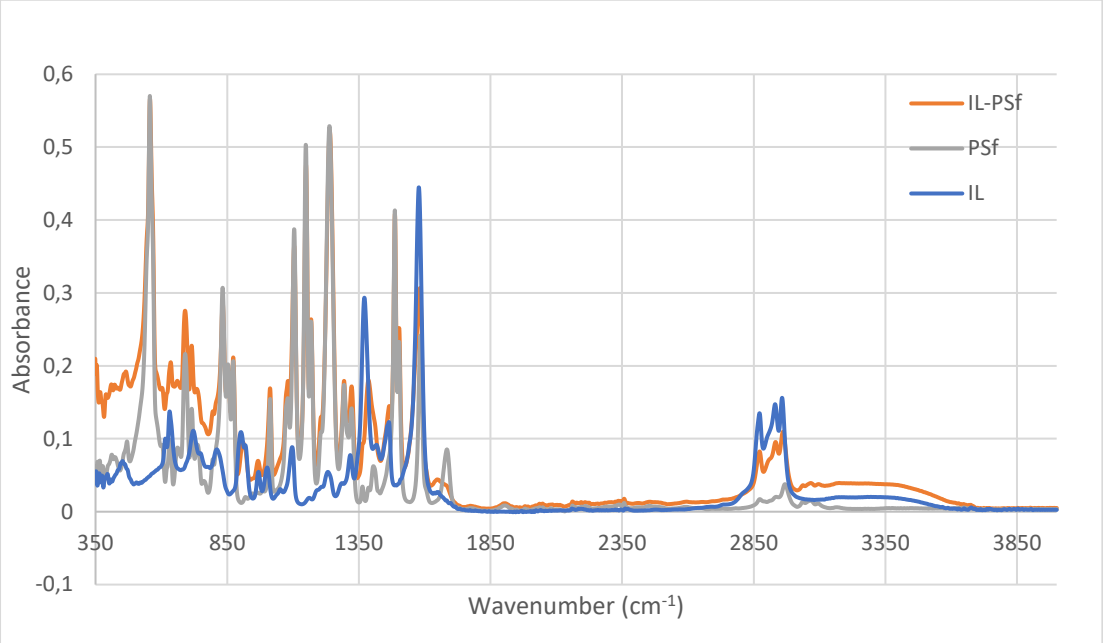

Figure 10. FTIR spectra for polysulfone (PSf) and ionic liquid impregnated polysulfone membranes (PSf-IL).